Solar Energy Materials & Solar Cells 100 (2012) 39–42

Contents lists available at ScienceDirect

Solar Energy Materials & Solar Cells

journal homepage: www.elsevier.com/locate/solmat

UV enhancement of silicon solar cells using thin SRO films

J. Carrillo-López [a], J.A. Luna-López [a], I. Vivaldo-De la Cruz [a,*], M. Aceves-Mijares [b], A. Morales-Sánchez [a], G. García-Salgado [a]

[a] CIDS-ICUAP, BUAP Ed. 103, Col, San Manuel. Puebla, Pue. 72570, México
[b] INAOE, Apdo. 51 Puebla, Pue. 72000, México

ARTICLE INFO

Article history:
Received 30 August 2010
Received in revised form
7 April 2011
Accepted 14 April 2011
Available online 6 May 2011

Keywords:
Solar cell
Silicon rich oxide
Silicon nanoparticles
Photoluminescence
Atomic force microscopy

ABSTRACT

A study of comparison of the electrical and optical characteristics of silicon solar cells (SC) with a layer of silicon oxide (SiO_2) deposited by SILOX, and silicon solar cells covered with a silicon rich oxide (SRO) film obtained by LPCVD containing silicon nanoparticles (Si-nps) was made. To increase the density of nanoparticles and thus improve the red photoluminescence, the SRO films were annealed at 1100 °C. Photoluminescence spectra and atomic force microscopy measurements of the silicon rich oxide films are presented and discussed, as well as current–voltage curves and spectral response of the fabricated solar cells. Measurement of the open circuit voltage and short circuit current of the SC under UV light illumination was realized. The results demonstrate that the red luminescence of these films with silicon nanoparticles, produces large enhancement of current and voltage, with improved performance in the UV range.

1. Introduction

Nowadays, photovoltaic (PV) energy is of the most attractive options for generating electricity using clean [1] and renewable energy. However, PV energy is not yet economical compared to energy obtained through conventional sources. Therefore, it is essential to reduce manufacturing costs of solar cells and photovoltaic modules. This can be achieved by improving the efficiency/cost ratio of solar cells, which constitute the photovoltaic modules [1–2].

The fundamental spectral losses in a single-junction solar cell made of semiconductor material such as silicon can be large. This is a result of the mismatch between the incident solar spectrum and the spectral absorption properties of the material [3]. Large parts of the solar spectrum are not absorbed, because of the existence of a band gap E_g of the material. Photons with energy E_{ph} larger than the band gap are absorbed, but the excess energy E_{ph}–E_g is not used effectively due to thermalization of the electrons, i.e. photons with $E_{ph} < E_g$ are not absorbed. Several routes have been proposed to overcome this intrinsic property of semiconductor solar cells and thereby increasing the power output of solar cells. All these methods or concepts concentrate on a much better use of the solar spectrum and are in general referred to as third generation photovoltaics [4].

One of the aims of this work was to increase the energy conversion efficiency of silicon solar cells by means of silicon rich oxide (SRO) films deposited on the SC surface. These films have the optical property of absorption below ~300 nm radiation (UV), so that the absorbed energy by the SRO film is then reemitted as red light (PL). Silicon SC have a greater response [5] in the spectral range from 500 to 1000 nm, so that the redshift of the short wavelengths offers an increase in the energy conversion efficiency of the silicon SC with no significant increase in the cost of fabrication.

In this paper, the electrical and optical parameters of silicon SC with SRO are compared with those for conventional SiO_2-covered silicon solar cells. One important point to mention is that the main interest of this work was just to study the photon-down conversion properties of SRO films, using as a reference a conventional SiO_2-covered silicon solar cell. SRO films were deposited by LPCVD technique. These films were annealed at 1100 °C for increasing the density of Si-nanoparticles and thus to increase the photoluminescence (PL) in the red wavelength range [6]. In previous papers [7–10] we have reported a study on SRO films regarding silicon excess and density as well as Si-nanoparticles size. It was possible to see silicon nanocrystals (Si-nc) in SRO_{10}, SRO_{20} (silicon excess of 10% and 6.5%, respectively) and amorphous silicon nanoclusters in SRO_{30} films (silicon excess of 4%) with diameters of approximately 5, 2.5 and 1 nm, respectively. In this work SRO_{30} films were used. PL spectra and atomic force microscopy (AFM) images corresponding to SRO films are presented and discussed, as well as current–voltage (*I–V*) curves and spectral response of the solar cells fabricated.

* Corresponding author. Tel.: +52 222 229 5500x7876.
E-mail addresses: jecarril@siu.buap.mx (J. Carrillo-López), israelvivac@gmail.com.mx (I. Vivaldo-De la Cruz).

0927-0248/$ - see front matter © 2011 Elsevier B.V. All rights reserved.
doi:10.1016/j.solmat.2011.04.029

2. Experiment details

SRO and SiO_2 were deposited on p-type silicon (1 0 0) substrates with resistivity of 9.5 Ω-cm, and 2 in. of diameter. The Si wafers were cleaned with standard cleaning processes RCAI and RCAII and rinsed in deionized water. The native oxide was removed from the Si wafers by a diluted HF dip (5%) for 10 s. The structures of the solar cells designed are similar to the conventional cells with SiO_2; the only difference in this case is the SRO top layer instead of the SiO_2 layer. Before the SRO deposit, the surface of the silicon wafers was textured with potassium hydroxide (KOH) anisotropic attack for 21 min at 85 °C. Fig. 1 shows the image of the textured surface; this is done in order to reduce the light reflection on the surface of the solar cell, which can be up to 30%. Subsequently, the diffusion of phosphorus was realized at 875 °C for 30 min for the formation of the n region and thus obtaining the p–n junction. SRO films were obtained in a horizontal LPCVD hot-wall reactor using SiH_4 (silane) and N_2O (nitrous oxide) as reactive gases at 715 °C. The gas flow ratio, $Ro=[N_2O]/[SiH_4]$, was used to control the amount of silicon excess in the SRO films. The surface of one group of solar cells (P1, P2, P3, P4) was passivated using SRO with two different thicknesses. Two other cells (P5, P6) were covered with thermal SiO_2 deposited by SILOX; then, an annealing at 1100 °C for two different times was applied to all the samples, as indicated in Table 1.

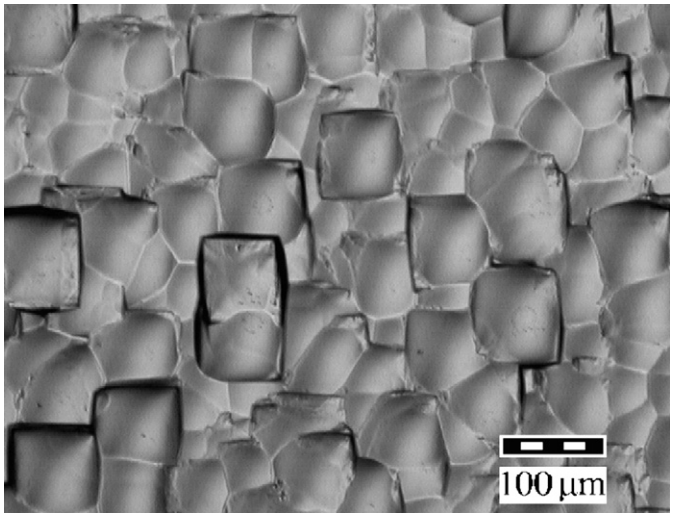

Fig. 1. Photograph of the silicon surface textured by anisotropic KOH attack.

Table 1
Solar cells with diferent annealing time and thickness of SRO and SiO_2.

		P1	P2	P3	P4	P5	P6
SRO (nm)	80	X	X				
	500			X	X		
Time annealed at 1100 °C (min)	90	X		X		X	
	180		X		X		X
SiO_2 (nm)	500					X	
	400						X

The annealing at 1100 °C is performed with two purposes, one is the formation of silicon nanoparticles embedded in the oxide matrix (SRO) and the other is the phosphorus redistribution and thus to obtain an optimum junction depth in the SC. Finally, Aluminum grids were patterned on the SRO surface by evaporation and standard photo-lithography. The surface Al grid electrodes have several fingers on all samples. It is important to remark that the zones between fingers are covered by the SRO films.

The surface morphology of SRO films was studied using a Nanosurf EasyScan atomic force microscopy (AFM) system version 2.3 operated in noncontact mode. A scanned area of $4 \times 4\ um^2$ was used for each topographic image. Four different scans were done for each sample, showing good reproducibility. AFM images were analyzed using scanning probe image processor (SPIP) software [11]. Room temperature PL of the SRO films was measured using a spectrofluorometer Horiba Jobin Yvon FluroMax 3 model with a xenon source of 150 mW and a monochromator. The samples were excited using 290 nm radiation, and the emission signal was collected from 400 to 950 nm with a resolution of 0.3 nm.

Characteristic current–voltage (I–V) curves of the SC were obtained using a solar simulator and a curve tracer under AM1.5 conditions. Also, we obtained the current versus wavelengths (I–W) characteristic curves of the SC. Short circuit current and open circuit voltage of the SC were measured under illumination of a lamp FL15GER with a wide range in the UV.

3. Results

Fig. 2 shows the 3-D surface morphology of SRO films. The annealing time strongly influences the size and density of grains so that a longer time of thermal treatment provoked more roughness and higher grains on the SRO surface. Fig. 3 depicts results of the roughness analysis. It is clearly noted that with thermal treatment the roughness and diameter of the grains increases in both SRO and SiO_2 films. The results obtained by SPIP software corresponding to grain diameter are listed in Table 2. The average roughness $\langle S_a \rangle$ is defined in [12].

The red photoluminescence of the SRO films was used for increasing the number of photons reaching the active region of the SC with appropriate energy to be trapped. PL spectra of the

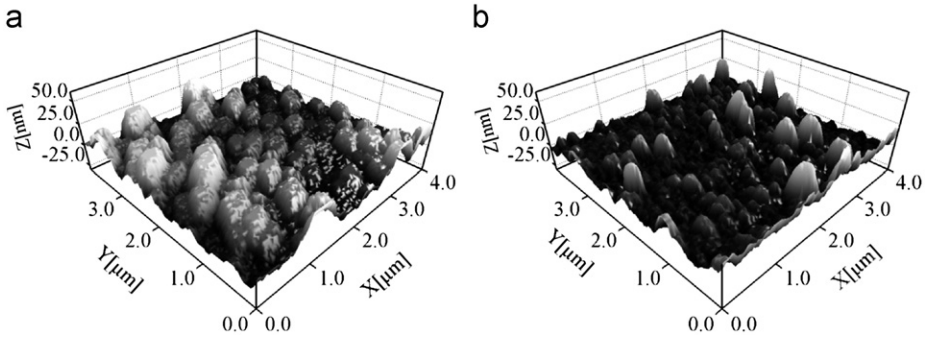

Fig. 2. 3-D image of SRO films annealed at 1100 °C for (a) 90 min and (b) 180 min.

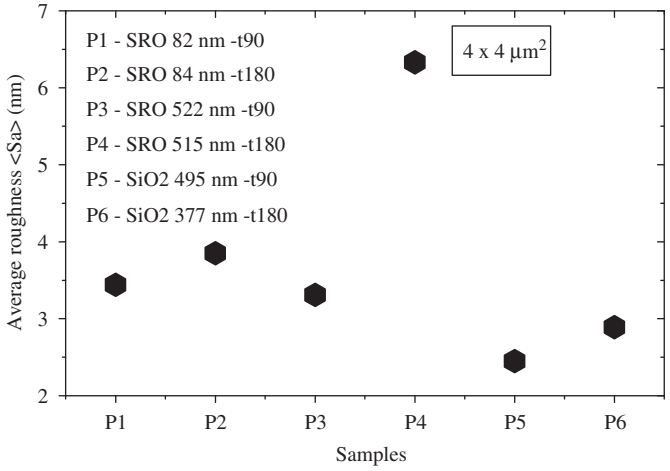

Fig. 3. Average roughness of the SRO and SiO_2 films.

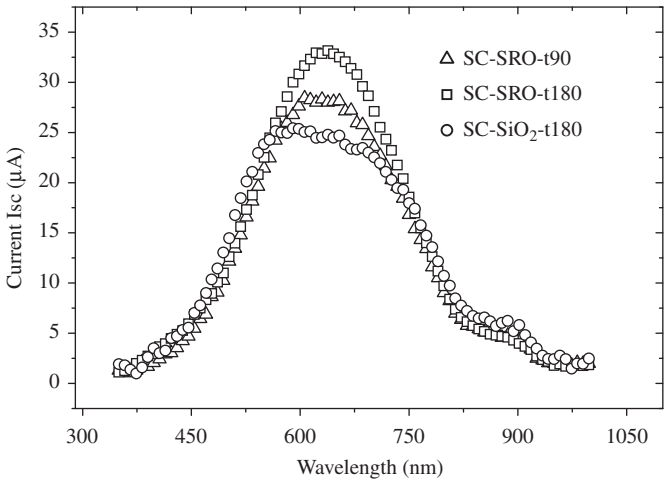

Fig. 5. Spectral response of solar cells with SRO and SiO_2 films.

Table 2
Characteristics of SRO films deposited on solar cells.

Sample	Thickness layer SRO (nm)	Time annealed at 1100 °C (min)	Grain diameter (nm)
P1	82	90	273
P2	84	180	250
P3	522	90	290
P4	515	180	443

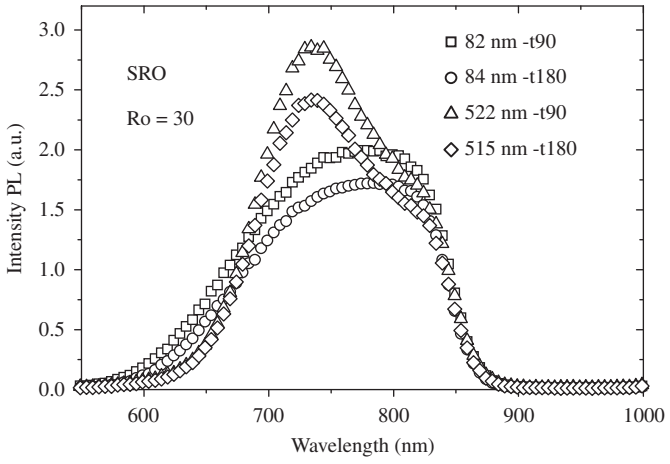

Fig. 4. Photoluminescence spectra of the SRO films deposited on the solar cell.

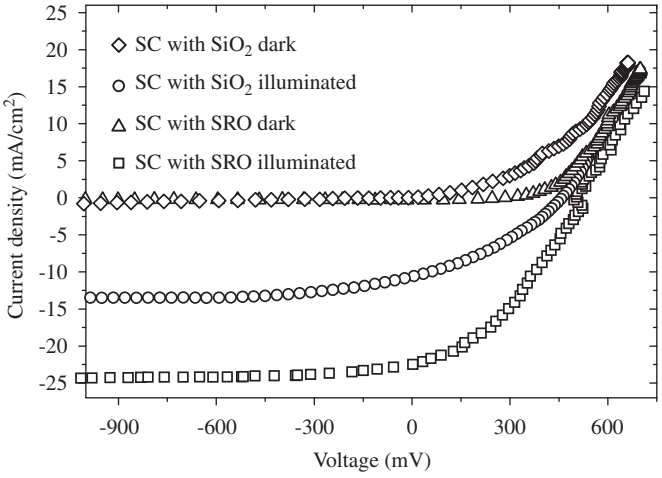

Fig. 6. *I–V* curves of SC with SRO and SiO_2 films.

Table 3
V_{oc} and I_{sc} of solar cells under illumination UV light.

Sample	Measurement	Dark	Illumination with UV light
P1	I_{sc} (μA)	0.03	728.0
	V_{oc} (mV)	0.00	120.0
P2	I_{sc} (μA)	0.04	1282.0
	V_{oc} (mV)	0.00	315.0
P5	I_{sc} (μA)	0.30	638.0
	V_{oc} (mV)	0.00	82.6
P6	I_{sc} (μA)	0.04	388.0
	V_{oc} (mV)	0.00	51.2

SRO films are shown in Fig. 4. It is clearly noted that the samples with the shorter annealing time show a higher PL intensity. As mentioned above, this PL reemitted as red light by the SRO film will reach the active region of the p–n junction, thus increasing the solar cell photocurrent.

Fig. 5 shows the spectral response in the visible and near infrared regions of the fabricated solar cells, where it is determined that the SC with SRO has a higher and better response than the cell with SiO_2. This fact confirms that the SRO is a material with good properties for applications in silicon solar cells technology.

I–V measurements from the silicon solar cells with SiO_2 and with SRO films are shown in Fig. 6. From these curves the open circuit voltage, short circuit current, fill factor and thus the maximum power can be obtained. These measurements were done using a solar simulator under AM1.5 conditions, and the *I–V* curves with the suitable hardware and software for the data processing. Table 3 presents V_{oc} and I_{sc} of solar cells under illumination with UV light. It is clearly noted that the solar cell with SRO (P2) has a better response to UV light.

4. Analysis and discussion

AFM images and measurements show that SRO films are rougher than silicon oxide films. The surface roughness of SRO

increases with the time of annealing; this is because the silicon excess in the SRO film forms silicon agglomerates and annealing at 1100 °C favors the formation of grains at the surface, as shown in Fig. 2. These results are consistent with those of other authors [12].

Photoluminescence of SRO films has been widely studied [6,13,14]. The two main mechanisms accepted for the generation of PL in the SRO, are the quantum confinement due to the nanocrystals, and defects present in the material. As shown above, SRO films show a high PL in the red. One point of view in favor of SRO films is that they have a transmittance greater than 80% for wavelengths greater than 400 nm, so that the material does not absorb radiation with wavelengths within the range from 500 to 1000 nm. This radiation is absorbed by silicon SC. Therefore, SRO films can be an excellent passivation material for SC, because they absorb short wavelength radiation (UV) and generate PL in the red region mainly, where the silicon SC has the larger spectral response. Also, as shown in Fig. 5, the solar cell covered with SRO (P2) has a better spectral response than the solar cell with SiO_2 (P5), in the visible and near-infrared regions. It should be noted that in the spectral response curve for the SRO-covered solar cell shown in Fig. 5, the contribution of current due to the photon-down conversion effect is not present; however, for comparison purposes with the spectral response for SiO_2-covered solar cells the graph is very useful. On the other hand, in the case of the *I–V* curves shown in Fig. 6, one additional component of current appears, since in the *I–V* measurement (AM1.5 conditions) the UV high energy photons are converted to low energy photons through the photon-down conversion effect. This statement becomes evident in the difference of short circuit currents shown in Fig. 6 for both types of solar cells.

From the characteristic *I–V* curves (Fig. 6) of the solar cells, the following best results were obtained: in the case of the cell passivated with SiO_2, it was found that $I_{sc}=10.6$ mA/cm^2 and $V_{oc}=455$ mV. From the cell covered with SRO the results were $I_{sc}=22.5$ mA/cm^2 and $V_{oc}=496$ mV. According to these values of short circuit current and open circuit voltage, when the cells are illuminated under AM1.5 conditions, the SRO-passivated solar cells show a higher I_{sc} and V_{oc} than the corresponding for the cells with SiO_2. For the purpose of proving the photon-down conversion effect present during the *I–V* measurements, both types of cells were illuminated with a high-energy excitation (blue–UV). The results of short circuit current and open circuit voltage are listed in Table 3. A current two times higher for the SRO-covered solar cell (P2) compared with that for the SiO_2-covered solar cell (P5) was measured. This improvement in current can be ascribed to absorption within Si-nps embedded in the oxide matrix [15]. Table 3 also shows an important increase in the open circuit voltage for the solar cell covered with SRO. This increase is directly related to the rise in photocurrent. One important point related to the photon-down conversion effect used in solar cells, is the fact that no shallow junctions are necessary for the solar cell structure, since the high energy photons are converted into red photons, which reach the active region of the junction. However, to get insight into the potential of such an effect more researching will be required.

From the point of view of solar cells applications, photoluminescence can be used for the improvement of efficiency in silicon solar cells. Photoluminescence can serve in the photon-down conversion process transforming the high energy-photons into lower-energy ones, in the range of red wavelengths, permitting an easier absorption by the silicon substrate and improving the cell's performance at high energies, which are usually lost by thermalization processes in conventional solar cells.

5. Conclusions

From the AFM measurements we concluded that the better value for I_{sc} corresponds to the P2 SRO film with a surface roughness of 3.85 nm and grain diameter of 250 nm. The silicon solar cells passivated with SRO indeed showed better results in spectral response than solar cell passivated with SiO_2 in the visible and near-infrared spectra. Solar cells covered with SRO show very high optical sensitivity for UV/blue region. The improvement in the spectral response and short circuit currents in the SRO-covered solar cells is due to the absorption of high-energy photons (UV) within the SRO film and the subsequent reemission of red light to the volume of the cell. Characteristic *I–V* curves of SRO-covered solar cells showed good results in open circuit voltage and short circuit current values, compared with those for the conventional SiO_2-covered solar cells. A current two times higher for the SRO-covered solar cell (P2) compared with that for the SiO_2-covered solar cell (P5) was measured when both types of cells are illuminated with a blue–UV light source.

Acknowledgments

We would like to thank Consejo Nacional de Ciencia y Tecnología (CONACYT) and VIEP-BUAP for providing support for this work.

References

[1] M.D. Archer, R. Hill (Eds.), Photoconversion of Solar Energy, Vol. 1, Clean Electricity from Photovoltaics, Imperial College Press, London, UK, 2001.
[2] M.A. Green, Third Generation Photovoltaics: Ultra-High Efficiency at Low Cost, Springer-Verlag, Berlin, Germany, 2003.
[3] K. Barnham, J.L. Marques, J. Hassard, P.O. Brien, Quantum dot concentrator and thermodynamic model for the global redshift, Appl. Phys. Lett. 76 (2000) 1197–1199.
[4] A.J. Chatten, K.W.J. Barnham, B.F. Buxton, N.J. Ekins-Daukes, M.A. Malik, A new approach to modelling quantum dot concentrators, Sol. Energy Mater. Sol. Cells 75 (2003) 363–371.
[5] L. Fahrenbruch, R.B. Bube, Fundamentals of Solar Cells, Photovoltaic Solar—Energy Convertion, Academic Press Inc, New York, 1983.
[6] F. Iacona, G. Franzo, C. Spinella, Correlation between luminiscence and structural properties of Si nanocrystals, J. Appl. Phys. 87 (2000) 1295–1303.
[7] J.A. Luna-López, M. Aceves-Mijares, O. Malik, Z. Yu, A. Morales, C. Dominguez, J. Rickards, Compositional and structural characterization of silicon naoparticles embedded in silicon rich oxide, Rev. Mex. Fís. S 53 (7) (2007) 293–298.
[8] A. Morales-Sanchez, J. Barreto, C. Domínguez-Horna, M. Aceves-Mijares, J.A. Luna-López, Optical characterization of silicon rich oxide, Sensors Actuators A 142 (2008) 12–18.
[9] Ragnar Kiebach, José Alberto Luna-López, Guilherme Osvaldo Dias, Mariano Aceves-Mijares, Jacobus Willibrordus Swardt, Characterization of silicon rich oxide with tunale optical band gap on sapphire substrates by photoluminescence, UV/Vis and Raman spectroscopy, J. Mex. Chem. Soc 52 (3) (2008) 212–218.
[10] Zhenrui Yu, M. Aceves-Mijares, A. Luna-López, Jinhui du, Dongcai Bian, Formation of silicon nanoislands on crystalline silicon substrates by thermal annealing of silicon rich oxide deposited by low pressure chemical vapor deposition, Nanotechnology 17 (2006) 4962–4965.
[11] J.F. Jogensen, SPIP, The Scanning Probe Image Processor, Denmark, 2002, 〈www.imagemet.com〉.
[12] J.A. Luna- López, A. Morales-Sánchez, M. Aceves-Mijares, Z. Yu, C. Domínguez, Analysis of surface roughness and its relationship with photoluminescence properties of silicon-rich oxide films, J. Vac. Sci. Technol. 27 (1) (2009) 57–62A 27 (1) (2009) 57–62.
[13] L.T. Canham, Silicon quantum wire array fabrication by electrochemical and chemical dissolution of wafers, Appl. Phys. Lett 57 (10) (1990) 1046–1048.
[14] H.Z. Song, X.M. Bao, N.S. Li, J.Y. Zhang, Relation between electroluminescence and photoluminescence of Si^+-implanted SiO_2, J. Appl. Phys. 82 (1997) 4028–4032.
[15] V. Svrcek, A. Slaoui, J.-C. Muller, Silicon nanocrystals as light converter for solar cells, Thin Solid Films 451–452 (2004) 384–388.